Role of multilevel Rydberg interactions in electric-field-tuned Förster resonances

Jorge M. Kondo, Donald Booth, Luís F. Gonçalves, James P. Shaffer, and Luis G. Marcassa

The role of multi-level Rydberg interaction in electric field tuned Förster resonances

Jorge M. Kondo[1], Donald Booth[2], Luís F. Gonçalves[1], James P. Shaffer[2] and Luis G. Marcassa[1*]

[1]*Instituto de Física de São Carlos, Universidade de São Paulo,*
Caixa Postal 369, 13560-970, São Carlos, SP, Brasil
[2]*Homer L. Dodge Department of Physics and Astronomy,*
The University of Oklahoma, 440 W. Brooks St., Norman, OK 73019, USA
(Dated: December 17, 2015)

In this work, we investigate the dc electric field dependence of 2 Förster resonant processes in ultracold ^{85}Rb, $37D_{5/2} + 37D_{5/2} \rightarrow 35L(L = O, Q) + 39P_{3/2}$, as a function of the atomic density. At low densities, the $39P_{3/2}$ yield as a function of electric field exhibits resonances. With increasing density, the linewidths increase until the peaks merge. Even under these extreme conditions, where the Förster resonance processes show little electrical field dependence, the $39P_{3/2}$ population depends quadratically on the total Rydberg atom population, suggesting that a 2-body interaction is the dominant process. In order to explain our results, we implement a theoretical model which takes into account the multi-level character of the interactions and Rydberg atom blockade process using only atom pair interactions. The comparison between the experimental data and the model is very good, suggesting that the Förster resonant processes are dominated by 2-body interactions up to atomic densities of $3.0 \times 10^{12}\,\mathrm{cm}^{-3}$.

It is not surprising that a central goal of ultracold Rydberg atom physics has been to investigate many-body physics because important parameters, such as density and interaction strength, can be controlled [1, 2]. A significant number of puzzling experimental observations in ultracold Rydberg gases have been explained by invoking many-body effects. Increasing the range of the atom-atom interactions is a natural pathway to study many-body physics. In this context, Förster resonances are the work horse for investigating many-body behavior in ultracold Rydberg gases. Recently, Förster resonances have attracted significant interest in the study of quantum systems driven by classical fluctuations [3], all-optical quantum information processing [4–6]; and quantum magnetism [7]. A detailed understanding of Förster resonances in high density samples is important to these lines of investigation.

Overviews of Förster resonance experiments can be found in several reviews [8–10]. Many works have associated Förster resonance broadening with many-body effects by comparing experimental observation to complex theoretical models. One such many-body model was implemented for the Rb states we study here [11]. More exact theoretical many-body approaches, like quantum Monte-Carlo, are difficult to implement in systems of highly excited atoms. A standard approximation involves breaking the multi-polar interactions between the atoms into a sum of 2-body problems [12–14].

It has been shown that 2-body potentials describing interactions between Rydberg atoms are very complex, particularly at short range where many interaction potentials cross. The potentials are sensitive to dc [15] and ac [16] electric fields. Studying a Förster resonance as a function of electric field and atomic density is generally complicated because essential quantities like state to state couplings and Rydberg atom blockade allowed interparticle separations change with applied electric field.

In this paper, we show, based on experiments and calculations of Rydberg atom potentials, that the multi-level character of the Rydberg atom interactions must be considered before concluding an experimental observation is many-body in nature. We define many-body here broadly to mean phenomena that involve the interaction of 3 or more atoms. For a system to exhibit many-body physics, the observables should be attributable to the many-body interactions. Rydberg atom blockade involves the collective behavior of more than 1 atom but the atoms do not interact with each other in pure blockade phenomena as the shared excitation prevents further excitation of the atoms within the blockade volume. In this sense, we distinguish purely collective phenomena from many-body interactions although the two are not mutually exclusive.

To demonstrate that the multi-level nature and complexity of Rydberg atom potentials is important for interpreting many-body behavior in ultracold Rydberg gases, we have studied the dc electric field dependence of 2 Förster resonance processes for ^{85}Rb atoms, $37D_{5/2} + 37D_{5/2} \rightarrow 35O(L = 11) + 39P_{3/2}$ and $37D_{5/2} + 37D_{5/2} \rightarrow 35Q(L = 12) + 39P_{3/2}$, as a function of the atomic density. The resonance peaks of the $39P_{3/2}$ state as a function of electric field can be clearly observed at MOT densities. However, as the density increases, the linewidth of the product yield increases until these peaks merge. Even under these extreme circumstances, where the Förster resonance processes do not show significant variation with electrical field, the $39P_{3/2}$ yield depends quadratically on the total Rydberg state population. As we have shown in our recent work [17], this is strong evidence that a 2-body interaction dominates the dynamics. We show that the multi-state nature of the Rydberg atom pair interaction potentials [15, 18, 19] can be used to explain the observed line broadening while maintaining consistency with the quadratic scaling of the product yield with Rydberg state

population. The explanation of the line broadening spectra at high densities requires that Rydberg atom blockade be taken into account [20, 21], but does not require the introduction of more than a 2-body interaction between a pair of atoms. Such results can be contrasted with the interpretation proposed in other works appearing in the literature [11, 14]. The experimental data and model agree well, suggesting, despite exciting a Förster resonance, the gas dynamics are dominated by 2-body interactions and the complexity of Rydberg interactions can mask the manifestation of many-body interactions.

The experimental setup is described elsewhere [17]. Briefly, a magneto-optical trap is used to load a quasi-electrostatic trap (QUEST), producing a non-polarized atomic sample of $\sim 10^6$ atoms at a peak density of $3.0 \pm 1.0 \times 10^{12} \, \mathrm{cm}^{-3}$ at a temperature of $80 \, \mu\mathrm{K}$. To probe the Rydberg atom interactions as a function of density, the QUEST is turned off and the sample undergoes free expansion which can vary from $0.1 - 1 \, \mathrm{ms}$. The atomic density for different free expansion times was verified by taking absorption images of the expanding atomic cloud. At t=0, the QUEST has a cigar shape with 35 microns radius and a length of 1450 microns. The Rydberg excitation occurs after free expansion using two narrow-bandwidth CW laser pulses at $\sim 780 \, \mathrm{nm}$ and $480 \, \mathrm{nm}$, whose duration is $700 \, \mathrm{ns}$, polarized parallel to the dc electric field. The intensities are $I_{780} = 1.6 \, \mathrm{mW \, cm}^{-2}$ and $I_{480} = 80 \, \mathrm{W \, cm}^{-2}$, and the respective peak Rabi frequencies are 19 and 29 MHz. To collect the Rydberg atom signal a ramped pulsed electric field is applied $70 \, \mathrm{ns}$ after the excitation. The electrons are counted on a multichannel plate detector; which gives an average Rydberg atom number of about 15,000. The uncertainty in the dc electric field is estimated to be $\sim 40 \, \mathrm{mV \, cm}^{-1}$. The $37D_{5/2}$ and $39P_{3/2}$ populations are observed simultaneously using their arrival time at the detector. We found no evidence of free ions in the experiment. By analyzing the electron signal at early times, we estimate that there are at most 4 free ions at the highest atomic density.

As in our prior work [17], we use a state-mixing fraction to analyze the population transfer from $37D_{5/2}$ to $39P_{3/2}$, similar to ref. [22]. However, we have defined our state-mixing fraction as twice the $39P_{3/2}$ electron signal divided by the sum of the $37D_{5/2}$ electron signal plus the $39P_{3/2}$ electron signal. The fraction is defined in this way because the $35O$ or $35Q$ electron signal contaminates the $37D_{5/2}$ electron signal in our experiment. The state-mixing fraction calculated in this way can lead to an overestimate of the experimental quantity relative to theory if some of the high l state was not measured in the $37D_{5/2}$ time-of-flight window. In Fig. 1, we show the dc electric field dependence of the state-mixing fraction as a function of the atomic density. The lowest density measurement was done in a MOT. As the atomic density increases, the linewidth as a function of electric field increases and the peaks, clearly visible at low density,
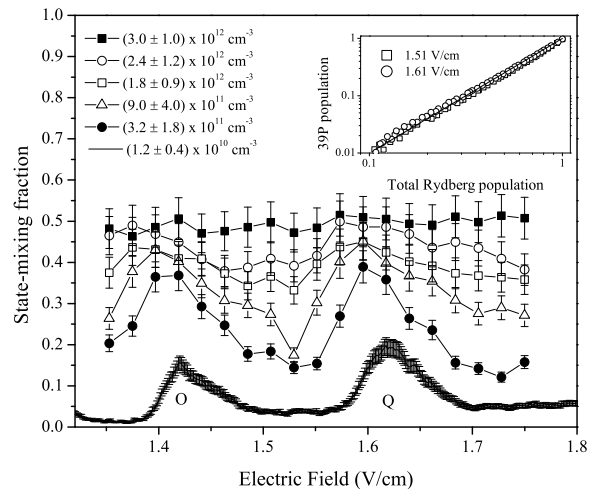

FIG. 1. State-mixing fraction as a function of dc electric field as a function of the atomic density. The resonances involving $L = O, Q$ are labeled. In the inset, we show the normalized $39P_{3/2}$ population as a function of the normalized total Rydberg atomic population for two different electric fields, off resonance at $1.51 \, \mathrm{V \, cm}^{-1}$ and on resonance at $1.61 \, \mathrm{V \, cm}^{-1}$.

merge. At the highest atomic density, the state-mixing fraction is almost independent of electric field. One might expect to observe many-body effects as this occurs.

A measurement of the atomic density dependence of the $39P_{3/2}$ population will show a power law dependence higher than 2 if multi-particle interactions are occurring [23]. In the inset of Fig. 1, we show the normalized $39P_{3/2}$ population as a function of normalized total Rydberg atomic population for 2 different electric fields. One electric field corresponds to off Förster resonance, $1.51 \, \mathrm{V \, cm}^{-1}$, and one to on resonance, $1.61 \, \mathrm{V \, cm}^{-1}$. The power law fit to the total Rydberg atom population, ρ^δ, is clearly second order as $\delta = 2.0 \pm 0.1$. It is clear from this straightforward data and analysis that the observed Förster resonance process is the result of a 2-body effect.

To explain the population transfer to $39P_{3/2}$, we calculated Rydberg atom interaction potential curves for $37D_{5/2} + 37D_{5/2}$ at fields around $1.65 \, \mathrm{V \, cm}^{-1}$ and performed an analysis on these potential curves to determine the expected lineshapes and product yields at various ground state atomic densities. At a field of $1.65 \, \mathrm{V \, cm}^{-1}$ ($1.45 \, \mathrm{V \, cm}^{-1}$), the asymptote corresponding to $39P_{3/2} + 35Q$ ($39P_{3/2} + 35O$) is degenerate with the $37D_{5/2} + 37D_{5/2}$ asymptote, enabling strong interactions which can result in population transfer. There is a small discrepancy between the experimental peak ($\sim 1.61 \, \mathrm{V \, cm}^{-1}$) and the theoretical one ($\sim 1.65 \, \mathrm{V \, cm}^{-1}$). The offset may be due to the small background electric field and/or a small offset resulting from the quantum defects used to calculate the energy levels. The interaction potential calculation for this system must include all L states up to $L = (n-1)$ [15]. For the $37D_{5/2} + 37D_{5/2}$
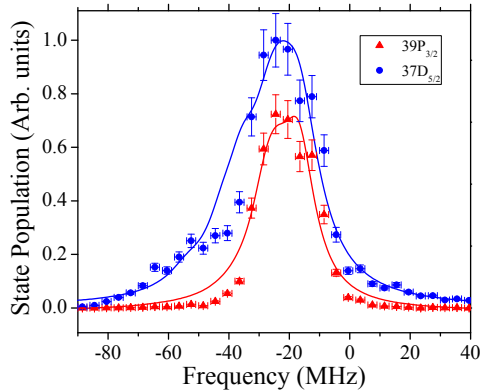
FIG. 2. (Color online) $37D_{5/2}$ and $39P_{3/2}$ state normalized populations as a function of the Rydberg excitation laser frequency on the Förster resonance at $1.61\,\mathrm{V\,cm^{-1}}$. The $37D_{5/2}$ state population shows saturation behavior, which is due to the Rydberg atom blockade. The points are the experimental data and the line is the theoretical model. The density for this measurement is $3 \times 10^{12}\,\mathrm{cm^{-3}}$. The signals are normalized to the peak $37D_{5/2}$ signal. No other free parameters are used to generate the theoretical graphs. The frequency 0 is set at the $37D_{5/2}$ atomic resonance at zero electric field.

system we calculated potentials and eigenvectors at fields varying from $1.35\,\mathrm{V\,cm^{-1}}$ to $1.65\,\mathrm{V\,cm^{-1}}$ in intervals of $0.025\,\mathrm{V\,cm^{-1}}$. At each of these fields we used the potentials and eigenvectors to calculate a lineshape for the $37D_{5/2}$ and $39P_{3/2}$ signals.

In prior work [17], we have demonstrated that a saturation behavior, which has been previously attributed to many-body effects [22], is actually a manifestation of the blockade effect due to two interacting atoms in a high density sample. We have verified that the $37D_{5/2}$ population saturates as the atomic density increases, consistent with the existence of a Rydberg atom blockade process. From this measurement, we are able to measure a Rydberg atom blockade radius of $5.3\,\mu\mathrm{m}$.

We calculate an absorption coefficient taking into account the saturation effects caused by Rydberg atom blockade to calculate the lineshape for the $37D_{5/2} + 37D_{5/2}$ signal and the $39P_{3/2}$ product yield. We use an absorption coefficient based on those found in [24, 25] as the starting point for the calculation:

$$\alpha(E) = \frac{\rho e^2 \pi}{4c\epsilon_0 m_e} \sum_{a=1}^{3} \frac{\sigma/2\pi}{\sigma^2 + (E_{dd_a} - E)^2} \quad (1)$$

$$\int_0^\infty \sum_i^{\text{all states}} P_{pair}(R) p_i(R) R^2 \mathrm{d}R. \quad (2)$$

$p_i(R)$ is the excitation probability into the $37D_{5/2} + 37D_{5/2}$ asymptotes E_{dd_a}, including each projection on the internuclear axis. For the $39P_{3/2}$ yield, the excitation probability contains an additional term indicating the overlap between $37D_{5/2} + 37D_{5/2}$ and $35O + 39P_{3/2}$ and $35Q + 39P_{3/2}$, $p_i(R) = p_P(R) p_D(R)$. e is the charge of the electron, ρ is the trap density and m_e is the mass of the electron. Since there is an applied electric field, the m_J sub-levels of $37D_{5/2} + 37D_{5/2}$ split, so it is important to account for each asymptote, a. E is the energy of the photon. σ is the spectral linewidth including the laser linewidth and the linewidth of $5P_{3/2}$. P_{pair} is the pair-state correlation function [18]. At the laser intensities and densities used in the experiment, saturation must be considered. The spectral lineshape with saturation is [26]

$$\alpha_{sat}(E) = \frac{\alpha(E)}{1 + S_E}, \quad (3)$$

where

$$S_E = \eta(\rho) \frac{B_{12} \rho_s(E)}{\Gamma} L(E_{dd_a} - E). \quad (4)$$

B_{12} is the Einstein coefficient of induced absorption, $\rho_s(E)$ is the spectral energy density of the excitation light, Γ is the mean relaxation rate, $\eta(\rho)$ is the hard sphere model parameter [27], and

$$L(E_{dd_a} - E) = \alpha(E) \frac{4c\epsilon_0 m_e}{\rho e^2 \pi} \quad (5)$$

is the lineshape function. The density-dependent hard-sphere model treats the system as spheres around the Rydberg atoms in which further excitation is forbidden. The hard sphere model accounts for the saturation of the lineshape due to Rydberg atom blockade. The region of electric fields between the crossings of $37D_{5/2} + 37D_{5/2}$ and $35O + 39P_{3/2}$ and $37D_{5/2} + 37D_{5/2}$ and $35Q + 39P_{3/2}$ was modeled and compared to experimental data.

The first test of the model is a comparison of the predicted frequency dependent excitation and product yield lineshapes obtained experimentally in a complementary experiment. The $37D_{5/2}$ and $39P_{5/2}$ populations were measured as a function of the Rydberg excitation laser frequency on the Förster resonance at $1.61\,\mathrm{V\,cm^{-1}}$ (Fig. 2). The trap density is $3 \times 10^{12}\,\mathrm{cm^{-3}}$. The agreement between theory and experiment is very good. We point out that: i) the model is able to reproduce the $39P_{3/2}/37D_{5/2}$ population ratio with no free parameter; ii) the small disagreement on the red side of the excitation lineshape can be explained by the fact the light polarization is not pure; and iii) if the Rydberg atom blockade effect is neglected, the $37D_{5/2}$ state population almost doubles around the resonance, showing that there is a strong saturation effect. The lineshape depends on the m_J of the asymptotic pair and thus the polarization of the excitation light. The structure observed in the lineshape is largely due to the splitting of the asymptotic pair states correlating to different m_J. We modeled the absorption lineshapes with the polarization to which
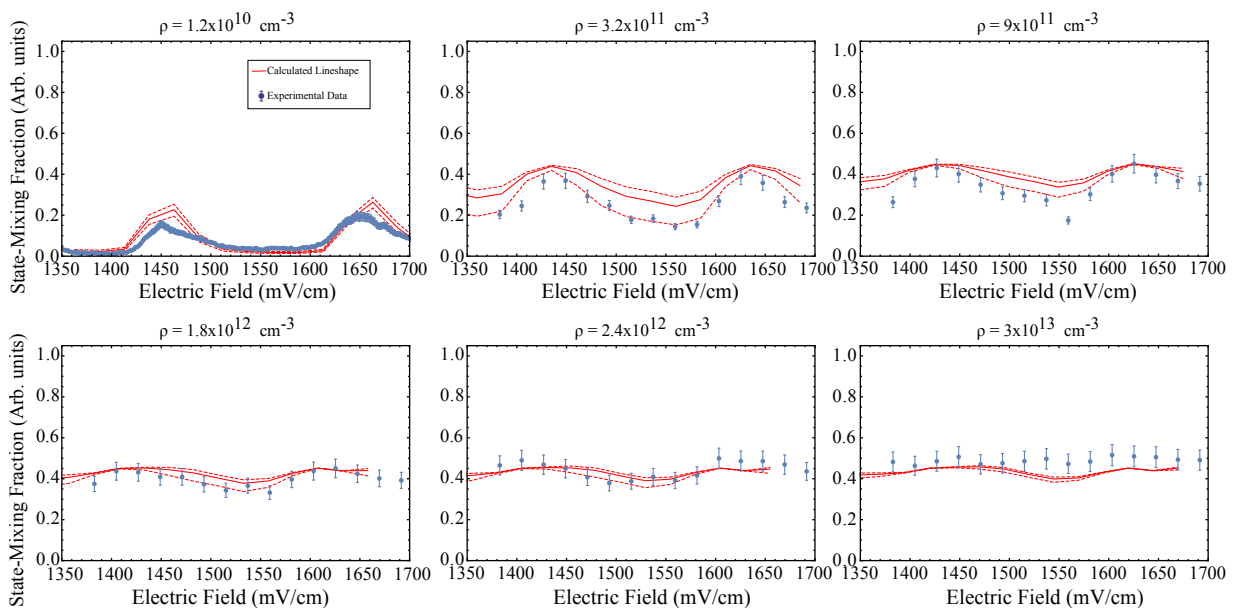
FIG. 3. (Color online) Experimental and calculated state-mixing fraction as a function of electric field, with an excitation laser detuning of 0 MHz from the $37D_{5/2}$ resonance at densities ranging from 1.2×10^{10} cm^{-3} to 3×10^{12} cm^{-3}. Two resonances appear in the density range shown; as the density is increased these resonances merge. The dashed lines represent the lower and upper boundary of the atomic density uncertainty.

the lasers were set. Polarization impurity can be introduced at the trap because of birefringence in the vacuum chamber windows and other optics. Rather than fitting the lineshape to a variable degree of ellipticity, we leave this effect as a systematic error to present the analysis without the elipticity as a free parameter.

In a second test, we reproduced the dc electric field dependence of the Förster resonance processes as a function of the atomic density. Fig. 3 shows the experimental and calculated state-mixing fraction as a function of electric field with a constant excitation laser detuning of 0 MHz from $37D_{5/2} + 37D_{5/2}$ at zero electric field at densities of 1.2×10^{10} cm^{-3}, 3.2×10^{11} cm^{-3}, 9.0×10^{11} cm^{-3}, 1.8×10^{12} cm^{-3}, 2.4×10^{12} cm^{-3}, and 3×10^{12} cm^{-3}. As the density increases, the lines broaden and the state-mixing fraction saturates to ~ 0.4 . At low density, the linewidth is due to a convolution of the: i) laser and state linewidths; and ii) multi-level nature of the potentials and the pair distribution function. The model predicts the linewidth for 1.2×10^{10} cm^{-3} primarily taking into account 2-body interactions. At high atomic density, the sample is blockaded. Outside the blockade radius the pair distribution function is basically constant and $p_i(R)$ has weak radial and electric field dependence.

The interpretation of these results is fairly straightforward. The system is dominated by pair interactions when the density is low enough so that interacting atoms are only excited in the asymptotic region where the interactions are weak. A third atom is, on average, so far

away from an interacting pair of atoms that there is no significant 3 or higher body interaction. As the density increases, Rydberg atom blockade prevents excitations from getting close enough to each other to begin to have significant 3 or higher body interactions. The multi-level nature of the Rydberg atom interaction potentials is more important than higher order interactions for explaining the lineshapes. The multi-level interaction potentials calculated in the electric field also tend to be weaker than what one would anticipate when these effects are not considered, at least around the $37D_{5/2} + 37D_{5/2}$ asymptote. Using idealized interaction potentials overestimates the strength of the interactions. Note that relatively weak excitation laser fields were used for our experiments. The multi-level effects explained here can also become relevant in strong laser fields [16].

In conclusion, we have studied the Förster resonance processes, $37D_{5/2} + 37D_{5/2} \rightarrow 35O + 39P_{3/2}$ and $37D_{5/2} + 37D_{5/2} \rightarrow 35Q + 39P_{3/2}$. We provided evidence that the broadening is not a many-body or even few-body effect. To explain our results, we implemented a model based on the multi-level character of 2-body interactions and Rydberg atom blockade. The model fits the experimental results well, supporting the explanation that the Förster resonance process, at least in this case, is dominated by a 2-body interaction. The complexity of Rydberg interactions can mask the manifestation of many-body behavior. Many-body or multi-particle effects should be proved through straightforward density scalings [23] or

other clear signatures such as nonlinear response.

ACKNOWLEDGMENTS

_____

[*] marcassa@ifsc.usp.br

[1] W. R. Anderson, J. R. Veale, and T. F. Gallagher, Phys. Rev. Lett. **80**, 249 (1998).

[2] I. Mourachko, D. Comparat, F. de Tomasi, A. Fioretti, P. Nosbaum, V. M. Akulin, and P. Pillet, Phys. Rev. Lett. **80**, 253 (1998).

[3] M. Sarovar and M. D. Grace, Phys. Rev. Lett. **109**, 130401 (2012).

[4] D. Paredes-Barato and C. S. Adams, Phys. Rev. Lett. **112**, 040501 (2014).

[5] D. Tiarks, S. Baur, K. Schneider, S. Dürr, and G. Rempe, Phys. Rev. Lett. **113**, 053602 (2014).

[6] D. Barredo, H. Labuhn, S. Ravets, T. Lahaye, A. Browaeys, and C. S. Adams, Phys. Rev. Lett. **114**, 113002 (2015).

[7] R. M. W. van Bijnen and T. Pohl, Phys. Rev. Lett. **114**, 243002 (2015).

[8] D. Comparat and P. Pillet, J. Opt. Soc. Am. B **27**, A208 (2010).

[9] T. F. Gallagher and P. Pillet, in *Advances in Atomic, Molecular and Optical Physics*, Advances In Atomic, Molecular, and Optical Physics, Vol. 56, edited by E. Arimondo, P. R. Berman, and C. C. Lin (Academic Press, 2008) p. 161.

[10] L. G. Marcassa and J. P. Shaffer, in *Advances in Atomic, Molecular and Optical Physics*, Advances In Atomic, Molecular, and Optical Physics, Vol. 63, edited by E. Arimondo, P. R. Berman, and C. C. Lin (Academic Press, 2014) p. 47.

[11] E. Altiere, D. P. Fahey, M. W. Noel, R. J. Smith, and T. J. Carroll, Phys. Rev. A **84**, 053431 (2011).

[12] J. V. Hernandez and F. Robicheaux, J. Phys. B **39**, 4883 (2006).

[13] B. Sun and F. Robicheaux, Phys. Rev. A **78**, 040701 (2008).

[14] T. J. Carroll, S. Sunder, and M. W. Noel, Phys. Rev. A **73**, 032725 (2006).

[15] A. Schwettmann, J. Crawford, K. R. Overstreet, and J. P. Shaffer, Phys. Rev. A **74**, 020701 (2006).

[16] V. A. Nascimento, L. L. Caliri, A. Schwettmann, J. P. Shaffer, and L. G. Marcassa, Phys. Rev. Lett. **102**, 213201 (2009).

[17] J. M. Kondo, L. F. Gonçalves, J. S. Cabral, J. Tallant, and L. G. Marcassa, Phys. Rev. A **90**, 023413 (2014).

[18] J. S. Cabral, J. M. Kondo, L. F. Gonçalves, L. G. Marcassa, D. Booth, J. Tallant, and J. P. Shaffer, New J. Phys. **12**, 093023 (2010).

[19] J. S. Cabral, J. M. Kondo, L. F. Gonçalves, V. A. Nascimento, L. G. Marcassa, D. Booth, J. Tallant, A. Schwettmann, K. R. Overstreet, J. Sedlacek, and J. P. Shaffer, J. Phys. B **44**, 184007 (2011).

[20] M. Robert-de Saint-Vincent, C. S. Hofmann, H. Schempp, G. Günter, S. Whitlock, and M. Weidemüller, Phys. Rev. Lett. **110**, 045004 (2013).

[21] C. Ates, S. Sevinçli, and T. Pohl, Phys. Rev. A **83**, 041802 (2011).

[22] K. C. Younge, A. Reinhard, T. Pohl, P. R. Berman, and G. Raithel, Phys. Rev. A **79**, 043420 (2009).

[23] J. H. Gurian, P. Cheinet, P. Huillery, A. Fioretti, J. Zhao, P. L. Gould, D. Comparat, and P. Pillet, Phys. Rev. Lett. **108**, 023005 (2012).

[24] J. Stanojevic, R. Côté, D. Tong, E. E. Eyler, and P. L. Gould, Phys. Rev. A **78**, 052709 (2008).

[25] J. Deiglmayr, H. Saßmannshausen, P. Pillet, and F. Merkt, Phys. Rev. Lett. **113**, 193001 (2014).

[26] W. Demtröder, *Laser Spectroscopy: Basic Concepts and Instrumentation*, 3rd ed. (Springer-Verlag, New York, 2003).

[27] C. S. Hofmann, *Emergence of correlations in strongly interacting ultracold Rydberg gases*, Ph.D. thesis, University of Heidelberg (2013).